Acta Crystallographica Section C
Crystal Structure Communications
ISSN 0108-2701

A urea adduct of bis(hinokitiolato)-copper(II)

Douglas M. Ho

Princeton University, Department of Chemistry, Princeton, NJ 08544-1009, USA
Correspondence e-mail: doug32009@gmail.com

Received 31 July 2010
Accepted 4 September 2010
Online 17 September 2010

Bis(μ_2-3-isopropyl-7-oxocyclohepta-1,3,5-trien-1-olato)bis-[(3-isopropyl-7-oxocyclohepta-1,3,5-trien-1-olato)copper(II)]–urea–acetone (1/6/2), $[Cu_2(C_{10}H_{11}O_2)_4]\cdot 6CH_4N_2O\cdot 2C_3H_6O$, where 3-isopropyl-7-oxocyclohepta-1,3,5-trien-1-olate is the systematic name for the hinokitiolate anion, contains three novel structural features. First, it contains a bis(hinokitiolato)copper(II) dimer, $[Cu(hino)_2]_2$, unlike any other, demonstrating that linkage isomerism is another avenue by which $Cu(hino)_2$ can transmute from one form to another. Second, $[Cu(hino)_2]_2$ is hydrogen bonded to two urea molecules, indicating that hydrogen bonding cannot yet be discounted from any proposed mechanism of action for the antimicrobial and antiviral properties of bis(hinokitiolato)-copper(II). Finally, corrugated urea layers crosslinked by $[Cu(hino)_2]_2$ dimers are observed, suggesting that a new family of host–guest materials, *i.e.* metallo–urea clathrates, exists to challenge our understanding of crystal engineering and crystal growth and design. Selected details of the structure are that the $[Cu(hino)_2]_2$ dimers possess crystallographic inversion symmetry, the Cu atoms have square-pyramidal coordination geometries, the basal Cu—O bonds are in the range 1.916 (2)–1.931 (2) Å, the apical Cu—O bond length is 2.582 (2) Å, the hinokitiolate bite angles are in the range 83.41 (7)–83.96 (8)°, the urea–$Cu(hino)_2$ interactions have an $R_2^2(8)$ motif, and the urea layers result from the close packing of $R_8^6(28)$ 'butterflies' and $R_8^6(24)$ 'strips of tape'.

Comment

Hinokitiol (β-thujaplicin) is a natural product that was first isolated from *Chamaecyparis taiwanensis* (Nozoe, 1936) and subsequently found to possess antitumor, antibacterial, antifungal and insecticidal properties (Inamori *et al.*, 1993, 2000; Arima *et al.*, 2003; Morita *et al.*, 2003). Metal complexes of hinokitiol have also been synthesized and found to possess antiviral and antimicrobial properties (Miyamoto *et al.*, 1998; Nomiya *et al.*, 2009). Among the latter metal complexes, bis(hinokitiolato)copper(II) or $Cu(hino)_2$ is unique. In particular, two earlier comments about this bioactive substance have served as the inspiration for the current study, namely 'the unusual structural chemistry of Cu^{II} hinokitiol' (Barret *et al.*, 2002), and the observation that its 'CuO_4 core inhibits an interaction of O atoms linked to C1 and C2 atoms with microorganisms/protein' (Nomiya *et al.*, 2004).

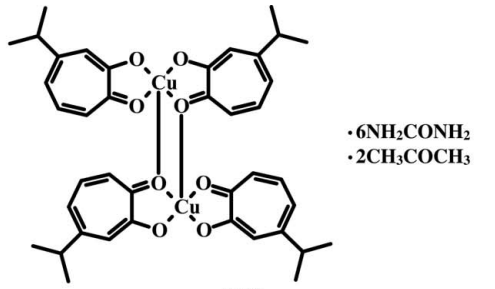

(IV)

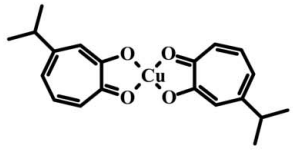

trans-Cu(hino)$_2$, (I)

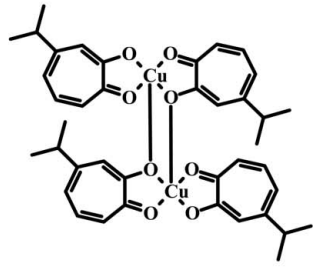

[*trans*-Cu(hino)$_2$]$_2$ in (II) (enoxy isomer)

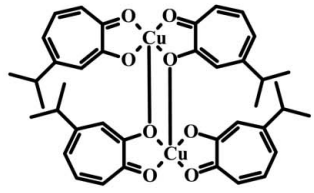

[*cis*-Cu(hino)$_2$]$_2$ in (II) and (III) (enoxy isomer)

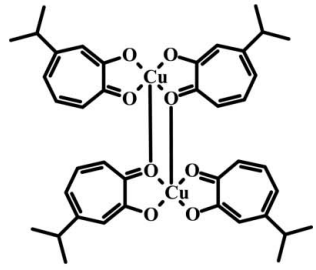

[*cis*-Cu(hino)$_2$]$_2$ in (IV) (keto isomer)

Historically, $Cu(hino)_2$ was first synthesized in 1936 (Nozoe, 1936) and large single crystals were clearly available by 1956 (Yamada & Tsuchida, 1956), but only much more recently, in 2002, was it finally subjected to X-ray diffraction by Molloy and co-workers and proclaimed to be somewhat 'unusual' (Barret *et al.*, 2002). $Cu(hino)_2$ has since been found to exist in six crystalline forms, *i.e.* modification (I) with four forms (Barret *et al.*, 2002; Nomiya *et al.*, 2004; Arvanitis *et al.*, 2004; Ho *et al.*, 2009), modification (II) with one form (Barret *et al.*, 2002) and modification (III) with one form (Ho, 2010), and its unusual structural diversity has so far been linked to *cis–trans* geometric isomerism, *syn–anti* conformational isomerism, aggregation *via* weak intermolecular Cu$\cdots\pi$ interactions, oligomerization *via* the hinokitiolate O atoms, and cocrystallization with other forms of itself.

A chloroform disolvate of modification (I) has also been structurally characterized and found to contain C—H$\cdots$O hydrogen bonds (Ho *et al.*, 2009). This latter observation is at

  doi:10.1107/S0108270110035602

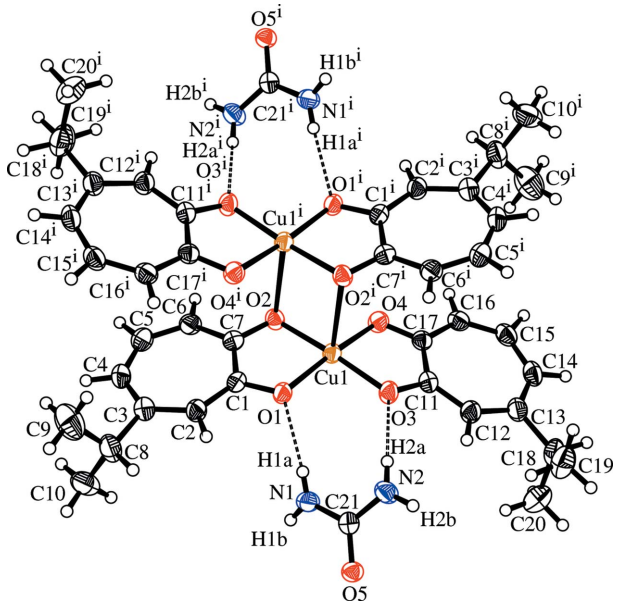

Figure 1
The [*cis*-Cu(hino)$_2$]$_2$ bis(urea) adduct in (IV). Dashed lines indicate hydrogen bonds, and displacement ellipsoids are drawn at the 50% probability level. The other unique urea and acetone solvent molecules have been omitted for clarity, as has the disorder in the isopropyl group at C8. [Symmetry code: (i) $-x+1, -y+1, -z+1$.]

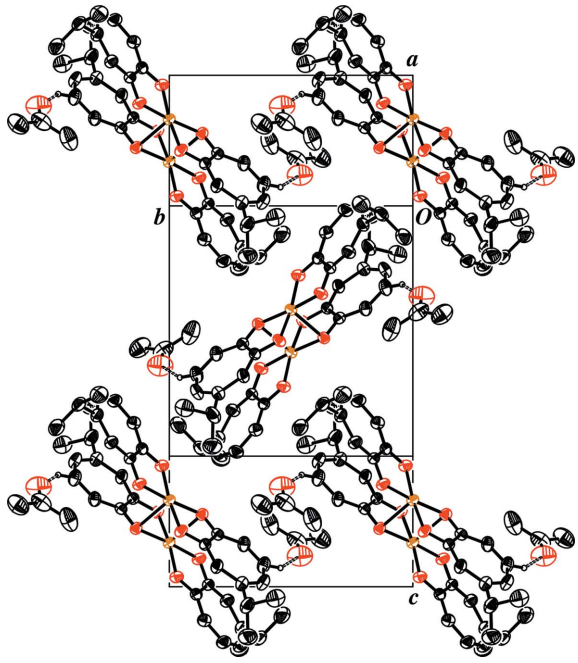

Figure 2
A projection diagram, normal to the (*h*00) family of planes, showing the packing and C5—H5···O8 hydrogen bonding (dashed lines) between the *cis*,*cis* dimers and acetone solvent molecules in (IV). Only those molecules intersecting with the $h = 2$ or (200) plane are shown. All other H atoms and the $h = 1$ or (100) plane populated solely by urea molecules have been omitted for clarity. Displacement ellipsoids are drawn at the 50% probability level.

odds with the earlier claim that protein–Cu(hino)$_2$ interactions, *e.g. via* N—H···O hydrogen bonding, are inhibited (Nomiya *et al.*, 2004). As a model for such an N—H···O interaction, a bis(urea) adduct analogous to the chloroform disolvate is both structurally and visually appealing and was pursued. An earlier unsuccessful attempt to isolate a urea adduct (Barret *et al.*, 2002) was re-examined by us and this time yielded [Cu(hino)$_2$]$_2$·6(urea)·2(acetone), (IV). The X-ray analysis of (IV), reported herein, provides the first unequivocal evidence and confirmation of urea adduct formation and N—H···O interactions with Cu(hino)$_2$. A view of the bis(urea) adduct in (IV) is given in Fig. 1, and selected geometric and hydrogen-bonding parameters are summarized in Tables 1 and 2, respectively.

As shown in Fig. 1, the targeted bis(urea) adduct of modification (I) was not obtained. Instead, a [Cu(hino)$_2$]$_2$ dimer was found. However, one quickly comes to appreciate that this unintended *cis*,*cis* dimer is unlike any other and is therefore a notable feature in and of itself. The *cis*,*cis* dimer has been observed only twice before, in modifications (II) and (III), and in both cases the enoxy O atoms of the hinokitiolate ligands were implicated in the dimerization (Barret *et al.*, 2002; Ho, 2010). This is also true in all known examples of [*M*(hino)$_2$*L*]$_2$ dimers (Nomiya *et al.*, 2009). The *cis*,*cis* dimer in (IV) is the one exception in which the keto O atoms are implicated instead. That the dimers in (II)–(III) and (IV) are linkage isomers of one another is evident in the reversal of selected distances and angles in Table 1. Hence, Cu1—O1 ≥ Cu1—O2 is observed for (II)–(III), but Cu—O1 < Cu1—O2 is observed with (IV). Similarly, O1—Cu1—O2^{i} < O2—Cu1—O2^{i} and O3—Cu1—O2^{i} < O4—Cu1—O2^{i} are observed for (II)–(III),

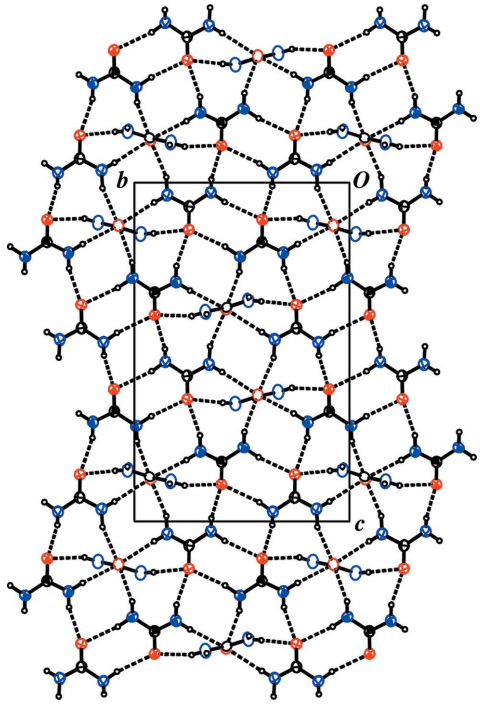

Figure 3
A projection diagram, normal to the *bc* plane, showing the hydrogen bonding (dashed lines) between urea molecules in (IV). Displacement ellipsoids are drawn at the 50% probability level. Boundary ellipses denote atoms O5, N1, N2 and C21, boundary and principal ellipses denote atoms O6, N3, N4 and C22, and octant-shaded ellipsoids denote atoms O7, N5, N6 and C23.

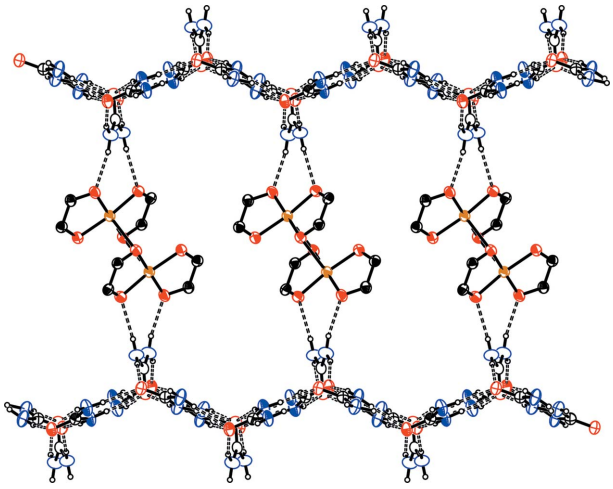

Figure 4
A projection diagram, showing the channels running parallel to [010] formed by crosslinking of the corrugated urea layers by the *cis*,*cis* dimers in (IV). Most of the hinokitiolate ligands and the acetone solvent molecules have been omitted for clarity. Dashed lines indicate hydrogen bonds, and displacement ellipsoids are drawn at the 50% probability level. Boundary ellipses denote atoms O5, N1, N2 and C21, boundary and principal ellipses denote atoms O6, N3, N4 and C22, and octant-shaded ellipsoids denote atoms O7, N5, N6 and C23.

while the opposite is noted for (IV) [symmetry code (i) for (II)–(IV) is $(-x+1, -y, -z)$, $(-x, -y, -z+2)$ and $(-x+1, -y+1, -z+1)$, respectively]. The torsion angles in Table 1 indicate that the full specifications for these dimers are (+*ac*,+*sp*),(−*ac*,−*sp*)-[*cis*-Cu(hino)$_2$]$_2$ for (II), (+*ap*,+*sp*),(−*ap*,−*sp*) for (III), and (+*ap*,−*sp*),(−*ap*,+*sp*) and (+*ac*,−*sp*),(−*ac*,+*sp*) for the major and minor conformers of (IV), respectively (Ho *et al.*, 2009). The *ap* and *ac* specifications for (IV) correspond to the major and minor components of a rotationally disordered isopropyl group at C8. Dimers (II)–(III) have (+,+),(−,−) conformations, *versus* (+,−),(−,+) for (IV), suggesting that the *syn* sign reversals may be a characteristic of linkage isomerism in these compounds as well. All three dimers have crystallographic inversion symmetry and bowed Cu(hino)$_2$ moieties, with those in (II)–(III) being more bowed than those in (IV) based on their C4···C14 distances, *i.e.* 11.176 (5) and 11.166 (6) Å *versus* 11.263 (4) Å, respectively.

The hydrogen bonding of a urea molecule to each Cu(hino)$_2$ moiety is the second notable feature of (IV) (Fig. 1). The graph-set motif for these urea–Cu(hino)$_2$ interactions is $R_2^2(8)$ (Etter, 1990; Etter *et al.*, 1990; Bernstein *et al.*, 1995). Surprisingly, while this motif is intuitively obvious, there are no other examples of it among α- or β-hydroxyketone transition metal complexes, and only two examples among unrelated ZnN_3O_3 and CoN_2O_4 systems, an aquahydroxyzinc(II) complex (Komen *et al.*, 1999) and a pivalatocobalt(II) dimer (Talismanova *et al.*, 2001). There are also no obvious trends in the O1—Cu1—O3 and O2—Cu1—O4 angles in (II)–(IV) that are attributable to the presence or absence of urea binding. For (IV), the O1—Cu1—O3 and O2—Cu1—O4 angles are 95.58 (8) and 96.20 (8)°, respectively, and the N1···O1 and N2···O3 distances are 2.944 (3) and 2.954 (3) Å, respectively.

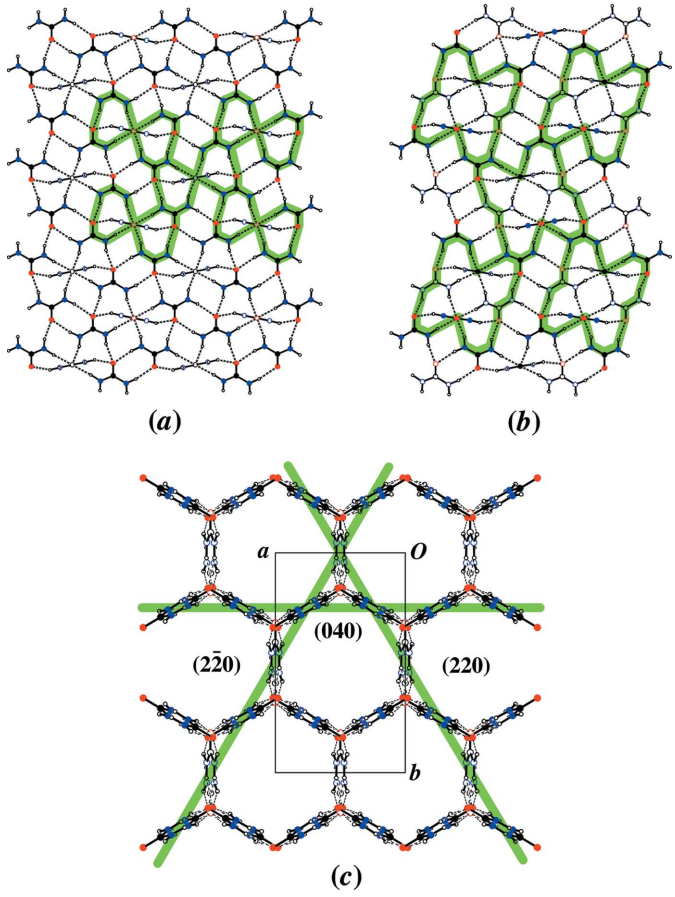

Figure 5
Projection diagrams for (V) viewed (*a*) normal to the (040) plane and (*b*) normal to the (220) plane, with packing motifs highlighted. In (*c*), the (040), (220) and (2$\bar{2}$0) planes are viewed edge-on and their locations shown by highlighted lines through them. The channels in (V) are completely specified by these three families of planes. The C and N atoms for the two unique urea molecules in (V) are indicated by filled and open spheres of arbitrary radii. All H atoms are shown as small open spheres for clarity.

For comparison, the O—*M*—O angle and N···O distances are 89.10 (13)° and 2.731 (6)–2.736 (6) Å, respectively, for the urea–Zn adduct, and 96.31 (13)° and 2.875 (4)–3.072 (5) Å, respectively, for the urea–Co adduct.

The third notable feature is recognizable at the unit-cell level, in that the crystal structure of (IV) is composed of layers of [Cu(hino)$_2$]$_2$ dimers and acetone solvent molecules (Fig. 2) alternating with layers of fully compacted urea molecules (Fig. 3). Each [Cu(hino)$_2$]$_2$ dimer is weakly linked to two acetone molecules *via* C5—H5···O8 interactions (graph set *D*) [C5—H5 = 0.95 Å, H5···O8 = 2.51 Å, C5···O8 = 3.313 (4) Å and C5—H5···O8 = 142°]. The hydrogen bonds within the urea layers are listed in Table 2. Each [Cu(hino)$_2$]$_2$ dimer also serves as a bridge or crosslink between the urea layers, yielding a three-dimensional host lattice with channels running parallel to the crystallographic *b* axis (Fig. 4). It is believed that (IV) is the only example of a metallo–urea clathrate in the truly classical sense.

The classic structures for urea inclusion compounds have been known since the mid-1900s (Schlenk, 1949; Smith, 1952).

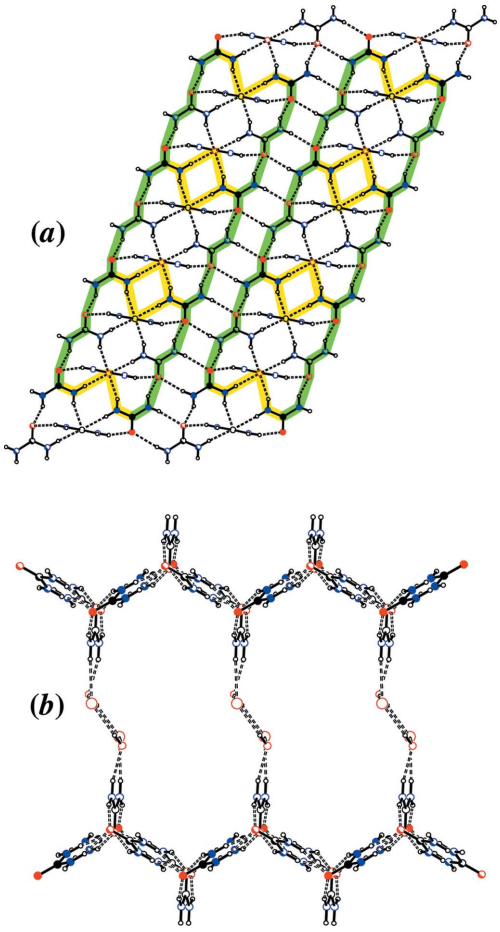

Figure 6
Projection diagrams of (*a*) the urea layers and (*b*) the channels in (VI). The packing motif in (*a*) is highlighted for comparison with the motifs in (V). The C and N atoms for the three unique urea molecules in (VI) are indicated by filled, shaded and open spheres of arbitrary radii. All H atoms are shown as small open spheres for clarity.

As examples, the host lattices for 1,4-dichlorobutane–urea, (V), and tetra-*n*-propylammonium bromide tris(urea) monohydrate, (VI), are shown in Figs. 5 and 6, respectively (Otto, 1972; Rosenstein *et al.*, 1973; Li & Mak, 1998). All classic urea clathrates contain fully compacted corrugated urea layers, and while other patterns of fully close-packed hydrogen-bonded urea molecules might be imagined, there are only three that have actually been observed (Figs. 5*a*, 5*b* and 6*a*). The pattern of Fig. 5(*a*) can be described as a close-packing of 'bow-ties' and short segmented 'strips of tape'. Each bow-tie is composed of two $R_2^2(8)$ and four $R_3^2(10)$ rings. The strips of tape are composed of a central $R_2^2(8)$ ring and two terminal $R_4^2(8)$ rings. For clarity, only the $R_3^2(10)$ rings normal to the viewer are highlighted, to show the motif of corner-sharing bow-ties. The pattern of Fig. 5(*b*) is just an alternate arrangement of the same $R_2^2(8)$, $R_3^2(10)$ and $R_4^2(8)$ rings, *i.e.* a close-packing of 'double bow-ties' or 'butterflies' and longer $R_8^6(24)$ strips of tape. Only the $R_8^6(28)$ rings are highlighted, to show the motif of corner-sharing butterflies. Finally, the pattern of Fig. 6(*a*) of alternating wide and narrow infinite strips of tape results from each butterfly sharing two wing-tips (rather than one) with each of its neighbors. The urea layer motif in (IV) (Fig. 3) is clearly synonymous with that shown in Fig. 5(*b*).

The hexagonal channels in a purely urea host lattice are the result of three sets of urea layers being oriented at roughly or exactly 120° with respect to each other (Fig. 5*c*). All three sets may possess the motif depicted in Fig. 5(*a*) (Schlenk, 1949; Smith, 1952), or the sets may be a mixture of two motifs (Figs. 5*a* and 5*b*), as shown for (V) (Otto, 1972). There are no examples with all three sets possessing the motif of Fig. 5(*b*). The peanut-shaped channels in (VI) are the result of a single set of urea layers being crosslinked by aggregates of two bromide anions and two water molecules (Fig. 6*b*) (Rosenstein *et al.*, 1973; Li & Mak, 1998). The channels in (IV) (Fig. 4) result from crosslinking with a transition metal complex instead, *i.e.* $[Cu(hino)_2]_2$, and are clearly analogous to those in (VI). The separations between urea layers are 7.08 (3), 14.559 (3) and 15.9471 (2) Å for (V), (VI) and (IV), respectively.

In summary, $[Cu(hino)_2]_2{\cdot}6(urea){\cdot}2(acetone)$, (IV), is a urea adduct of bis(hinokitiolato)copper(II). Urea–$Cu(hino)_2$ N—H···O hydrogen bonding has been confirmed, suggesting that the hinokitiolate O atoms are indeed available for microorganism/protein interactions, *e.g. via* the N—H group present in all peptide bonds and in arginine, asparagine, glutamine, histidine, lysine and tryptophan residues. Additionally, (IV) is also the only example of a classical metallo–urea clathrate. The clathrate urea layers are crosslinked by $[Cu(hino)_2]_2$ dimers and the dimers themselves are also unique, *i.e.* no other keto μ_2-O-bridged hinokitiolate dimers are known. The 'unusual structural chemistry of Cu^{II} hinokitiol' now includes linkage isomerism as yet another pathway for structural diversification.

Experimental

A small vial was charged with [*cis*-$Cu(hino)_2]_2{\cdot}$[*trans*-$Cu(hino)_2]_2{\cdot}$-*trans*-$Cu(hino)_2$, (II) (39 mg, 0.02 mmol), and urea (18 mg, 0.30 mmol). The solids were dissolved in acetone (5 ml), and the vial lightly capped to allow the solution to evaporate slowly at room temperature. Green needles and rectangular prisms of [*cis*-$Cu(hino)_2]_2{\cdot}$-$6(urea){\cdot}2(acetone)$, (IV), appeared within a few days. Crystals of (IV) desolvate upon standing in air, so the solution should not be allowed to evaporate to dryness. A needle and a prism were both examined and found to have the same unit cell. Both were also dichroic, appearing emerald green when viewed perpendicular to the 100 face and light green when viewed perpendicular to either the 011 or $01\bar{1}$ faces. As it was larger, a cut needle was selected for the diffraction experiment.

Crystal data

$[Cu_2(C_{10}H_{11}O_2)_4]{\cdot}6CH_4N_2O{\cdot}{\cdot}2C_3H_6O$
M_r = 1256.36
Monoclinic, $P2_1/c$
a = 17.0125 (2) Å
b = 11.0470 (2) Å
c = 17.2731 (3) Å
β = 110.385 (1)°
V = 3042.95 (8) Å^3
Z = 2
Mo $K\alpha$ radiation
μ = 0.77 mm^{-1}
T = 200 K
0.30 × 0.10 × 0.04 mm

Data collection

Nonius KappaCCD area-detector diffractometer
Absorption correction: multi-scan (*SCALEPACK*; Otwinowski & Minor, 1997)
T_{min} = 0.801, T_{max} = 0.973
41379 measured reflections
6996 independent reflections
4582 reflections with $I > 2\sigma(I)$
R_{int} = 0.074

Refinement

$R[F^2 > 2\sigma(F^2)]$ = 0.053
$wR(F^2)$ = 0.147
S = 1.06
6996 reflections
433 parameters
19 restraints
H atoms treated by a mixture of independent and constrained refinement
$\Delta\rho_{max}$ = 0.76 e Å^{-3}
$\Delta\rho_{min}$ = −0.63 e Å^{-3}

Table 1
Selected geometric parameters (Å, °).

For each isopropyl substituent, *X* corresponds to the centroid for each pair of methyl C atoms, *viz.* C9/C10, C9*/C10* and C19/C20 (Ho *et al.*, 2009).

	(II)†	(III)‡	(IV)§
Cu1—O1	1.933 (2)	1.931 (3)	1.9219 (19)
Cu1—O2	1.932 (2)	1.921 (3)	1.9310 (18)
Cu1—O3	1.920 (2)	1.915 (2)	1.9157 (18)
Cu1—O4	1.919 (2)	1.915 (3)	1.916 (2)
Cu1—O2^{i}	2.476 (2)	2.658 (3)	2.582 (2)
C4···C14	11.176 (5)	11.166 (6)	11.263 (4)
O1—Cu1—O2	83.26 (7)	83.49 (11)	83.41 (7)
O3—Cu1—O4	83.86 (7)	83.64 (10)	83.96 (8)
O1—Cu1—O2^{i}	86.92 (6)	86.26 (10)	102.09 (7)
O2—Cu1—O2^{i}	103.62 (7)	100.17 (9)	85.89 (7)
O3—Cu1—O2^{i}	90.79 (7)	85.62 (9)	99.60 (7)
O4—Cu1—O2^{i}	93.42 (7)	100.44 (10)	86.72 (7)
Cu1—O2—Cu1^{i}	93.09 (6)	93.74 (10)	94.11 (7)
C2—C3—C8—*X*/*X**	145.4 (7)	171.6 (5)	−178.6 (6)/ −147 (1)
C12—C13—C18—*X*	4.6 (4)	5.8 (4)	10.1 (4)

† The *cis*,*cis* dimer in Barret *et al.* (2002). ‡ Ho (2010). § This work. Symmetry code: (i) $-x+1, -y, -z$ for (II); $-x, -y, -z+2$ for (III); $-x+1, -y+1, -z+1$ for (IV).

The positional parameters for the urea H atoms were free to vary. All other H atoms were allowed to ride on their respective C atoms, with C—H = 0.95, 1.00 and 0.98 Å for the cycloheptatriene, methine and methyl H atoms, respectively, and with U_{iso}(H) = 1.2U_{eq}(C) for the cycloheptatriene and methine H atoms, 1.5U_{eq}(C) for the methyl H atoms and 1.5U_{eq}(N) for the urea H atoms. One of the isopropyl groups was rotationally disordered and was treated with a two-site model, C9/C10 and C9*/C10*, with refined site-occupancy factors of 0.66 (2) and 0.34 (2), respectively. Atom C8 is common to both components of the disorder. A total of 19 restraints were employed: C8—C9, C8—C10, C8—C9* and C8—C10* bond-length restraints of 1.524 (5) Å (4), C8—C9*, C8—C10* and C9*—C10* rigid-bond (DELU) restraints (3), and displacement ellipsoid similarity restraints (SIMU) applied to atoms C8, C9* and C10* (12) (software commands from *SHELXTL*; Sheldrick, 2008).

Data collection: *COLLECT* (Nonius, 1998); cell refinement: *DENZO*/*SCALEPACK* (Otwinowski & Minor, 1997); data reduction: *DENZO*/*SCALEPACK*; program(s) used to solve structure: *SHELXTL* (Sheldrick, 2008); program(s) used to refine structure: *SHELXTL*; molecular graphics: *SHELXTL* and *ORTEP-3* (Farrugia, 1997); software used to prepare material for publication: *SHELXTL*.

Table 2
Hydrogen-bond geometry for (IV) (Å, °).

D—H···*A*	*D*—H	H···*A*	*D*···*A*	*D*—H···*A*
N1—H1*A*···O1	0.80 (4)	2.15 (4)	2.944 (3)	175 (4)
N1—H1*B*···O6	0.78 (4)	2.17 (4)	2.951 (3)	178 (4)
N2—H2*A*···O3	0.84 (4)	2.13 (4)	2.954 (3)	167 (4)
N2—H2*B*···O7	0.83 (4)	2.27 (4)	3.079 (3)	164 (4)
N3—H3*A*···O5^{ii}	0.94 (4)	2.14 (4)	3.041 (3)	160 (3)
N3—H3*B*···O5	0.78 (4)	2.24 (4)	3.011 (3)	174 (4)
N4—H4*A*···O7^{ii}	0.80 (4)	2.11 (4)	2.901 (3)	168 (4)
N4—H4*B*···O7^{iii}	0.90 (4)	2.16 (4)	3.032 (3)	163 (3)
N5—H5*A*···O6^{iv}	0.84 (4)	2.09 (4)	2.901 (4)	164 (4)
N5—H5*B*···O5	0.86 (4)	2.16 (4)	3.007 (3)	169 (3)
N6—H6*A*···O5^{iv}	0.85 (4)	2.19 (4)	3.012 (3)	163 (3)
N6—H6*B*···O6^{v}	0.94 (4)	2.07 (4)	3.000 (3)	168 (3)

Symmetry codes: (ii) $-x, -y+1, -z+1$; (iii) $x, y-1, z$; (iv) $-x, y+\frac{1}{2}, -z+\frac{1}{2}$; (v) $x, y+1, z$.

The author extends sincere thanks to Dr Susan K. Byram (Bruker AXS) for software support and Dr Judith C. Gallucci (The Ohio State University) for helpful discussions.

Supplementary data for this paper are available from the IUCr electronic archives (Reference: EG3059). Services for accessing these data are described at the back of the journal.

References

Arima, Y., Nakai, Y., Hayakawa, R. & Nishino, T. (2003). *J. Antimicrob. Chemother.* **51**, 113–122.
Arvanitis, G. M., Berardini, M. E. & Ho, D. M. (2004). *Acta Cryst.* C**60**, m126–m128.
Barret, M. C., Mahon, M. F., Molloy, K. C., Wright, P. & Creeth, J. E. (2002). *Polyhedron*, **21**, 1761–1766.
Bernstein, J., Davis, R. E., Shimoni, L. & Chang, N.-L. (1995). *Angew. Chem. Int. Ed. Engl.* **34**, 1555–1573.
Etter, M. C. (1990). *Acc. Chem. Res.* **23**, 120–126.
Etter, M. C., MacDonald, J. C. & Bernstein, J. (1990). *Acta Cryst.* B**46**, 256–262.
Farrugia, L. J. (1997). *J. Appl. Cryst.* **30**, 565.
Ho, D. M. (2010). *Acta Cryst.* C**66**, m145–m148.
Ho, D. M., Berardini, M. E. & Arvanitis, G. M. (2009). *Acta Cryst.* C**65**, m391–m394.
Inamori, Y., Sakagami, Y., Morita, Y., Shibata, M., Sugiura, M., Kumeda, Y., Okabe, T., Tsujibo, H. & Ishida, N. (2000). *Biol. Pharm. Bull.* **23**, 995–997.
Inamori, Y., Tsujibo, H., Ohishi, H., Ishii, F., Mizugaki, M., Aso, H. & Ishida, N. (1993). *Biol. Pharm. Bull.* **16**, 521–523.
Komen, R. P., Miskelly, G. M., Oliver, A. & Rickard, C. E. F. (1999). *Acta Cryst.* C**55**, 1213–1215.
Li, Q. & Mak, T. C. W. (1998). *Acta Cryst.* B**54**, 180–192.
Miyamoto, D., Kusagaya, Y., Endo, N., Sometani, A., Takeo, S., Suzuki, T., Arima, Y., Nakajima, K. & Suzuki, Y. (1998). *Antiviral Res.* **39**, 89–100.
Morita, Y., Matsumura, E., Okabe, T., Shibata, M., Sugiura, M., Ohe, T., Tsujibo, H., Ishida, N. & Inamori, Y. (2003). *Biol. Pharm. Bull.* **26**, 1487–1490.
Nomiya, K., Onodera, K., Tsukagoshi, K., Shimada, K., Yoshizawa, A., Itoyanagi, T., Sugie, A., Tsuruta, S., Sato, R. & Kasuga, N. C. (2009). *Inorg. Chim. Acta*, **362**, 43–55.
Nomiya, K., Yoshizawa, A., Kasuga, N. C., Yokoyama, H. & Hirakawa, S. (2004). *Inorg. Chim. Acta*, **357**, 1168–1176.
Nonius (1998). *COLLECT*. Nonius BV, Delft, The Netherlands.
Nozoe, T. (1936). *Bull. Chem. Soc. Jpn*, **11**, 295–298.
Otto, J. (1972). *Acta Cryst.* B**28**, 543–551.

Otwinowski, Z. & Minor, W. (1997). *Methods in Enzymology*, Vol. 276, *Macromolecular Crystallography*, Part A, edited by C. W. Carter Jr & R. M. Sweet, pp. 307–326. New York: Academic Press.
Rosenstein, R. D., McMullan, R. K., Schwarzenbach, D. & Jeffrey, G. A. (1973). *Am. Crystallogr. Assoc. Abstr. Papers (Summer Meet.)*, p. 152.
Schlenk, W. (1949). *Justus Liebigs Ann. Chem.* **565**, 204–240.
Sheldrick, G. M. (2008). *Acta Cryst.* A**64**, 112–122.
Smith, A. E. (1952). *Acta Cryst.* **5**, 224–235.
Talismanova, M. O., Sidorov, A. A., Novotortsev, V. M., Aleksandrov, G. G., Nefedov, S. E., Eremenko, I. L. & Moiseev, I. I. (2001). *Izv. Akad. Nauk. SSSR Ser. Khim.* pp. 2149–2151.
Yamada, S. & Tsuchida, R. (1956). *Bull. Chem. Soc. Jpn*, **29**, 694–700.